Tether," Ph.D. Dissertation, Dept. of Aerospace Engineering, Indian Inst. of Technology, Kanpur, India, Aug. 1997.

G. D. Gamble
Associate Editor

Variable Attitude Compensation Through Tether for Comsats in Drifting/Inclined Geosynchronous Orbits

Krishna Kumar* and K. D. Kumar†
Indian Institute of Technology, Kanpur 208 016, India

Nomenclature

a_j	= x coordinate of attachment point j; is 0 for $j = 1, 2$ and $(-1)^j a$ for $j = 3, 4$
C	= $EA/(mL_{\text{ref}}\Omega_{\text{ea}}^2)$; TSS rigidity parameter
c_j	= z coordinate of attachment point j; is $(-1)^j a$ for $j = 1, 2$ and 0 for $j = 3, 4$
EA	= tether modulus of rigidity, N
I_x, I_y, I_z	= principal satellite moments of inertia about x, y, and z axes, respectively
i_b	= orbit inclination, deg
j	= tether points on satellite; 1, 2, 3, 4 for A, B, C, D, respectively
K_p	= inertia parameters: $p = 1, 2, \ldots, 5$; $K_1 = (I_x - I_y)/I_z$, $K_2 = (I_y - I_z)/I_x$, $K_3 = (I_x - I_z)/I_y$, $K_4 = 1 - K_1K_5$, $K_5 = (K_3 - 1)/(K_1K_3 - 1)$
L_j, L_{j0}	= stretched and nominal unstretched length of jth tether, respectively
L_{ref}	= reference length; $(I_x/m)^{1/2}$
L_{t0}	= nominal unstretched lengths of four tethers
L_0	= L when tether strains are zero
l, l_j, l_{j0}, l_{t0}	= L/L_{ref}, L_j/L_{ref}, L_{j0}/L_{ref}, and L_{t0}/L_{ref}, respectively
$U(\epsilon_j)$	= 1 for $\epsilon_j \geq 0$ and 0 for $\epsilon_j < 0$
ϵ_j	= tether strains in the jth tether
λ_j	= Lagrange multipliers
Ω_{ea}	= spin velocity of the Earth
$(\hat{\ })$	= $(.)/L_{\text{ref}}$
$(.)_j$	= (.) for jth tether; $j = 1, 2, 3, 4$ for tethers $E-A$, $E-B$, $E-C$, $E-D$
$(.)_0$	= (.) at θ(true anomaly) = 0
$\lvert(.)\rvert_{\max}$	= maximum amplitude of (.)
$(.)'$, $(.)''$	= $\mathrm{d}(.)/\mathrm{d}\theta$ and $\mathrm{d}^2(.)/\mathrm{d}\theta^2$, respectively

Introduction

THE geostationary communications satellites undergo significant continual changes in their orbital elements under the influence of environmental perturbations. Of these, the adverse secular effect on the orbital inclination is of considerable practical importance. It causes the satellites to undergo continually growing periodic lateral/longitudinal satellite drifts as viewed from the ground terminal. Rather expensive onboard fuel is periodically utilized for station-keeping maneuvers to ensure continual, uninterrupted communications. Here, it is proposed to explore the feasibility for developing a variable attitude controller using tethered auxiliary mass for continual satellite tilting so as to effectively compensate for the periodic longitudinal and lateral drifts for satellites in 24-h nonequatorial circular orbits with respect to an equatorial ground station. This study is based on results of some earlier investigations[1–7] that have established the effectiveness of the tethered satellite system (TSS) for satellite attitude stabilization and maneuver. In the light of the rapid worldwide growth in demands on communications capacity, extension of the satellite applications to new areas such as information technology and the associated problems of excessive overcrowding of the geostationary ring,[8–10] this investigation may be of considerable significance.

Proposed Controller Model and Equations of Motion

This investigation considers a satellite moving in a nonequatorial, 24-h orbit. The satellite is assumed to be vertically above the ground station while passing over the nodes (Fig. 1). The line through the ascending node represents the reference line in orbit for measurement of the true anomaly θ. The coordinate frame x_0, y_0, z_0, passing through the system center of mass S with y_0 pointing along the local vertical and x_0 along the normal to the orbital plane, represents the local orbital reference frame. Three successive rotations of this local frame, α (pitch), γ (yaw), and ϕ (roll), lead to the general satellite orientation represented by its body frame $S - xyz$.

The proposed satellite controller model is composed of an auxiliary mass deployed using four identical tethers attached to four distinct points on satellite surface (Fig. 1). The attachment points lie in a plane parallel to the satellite-yaw plane in a symmetric pattern with the xyz coordinates given as $A \equiv (0, -b, a)$, $B \equiv (0, -b, -a)$, $C \equiv (-a, -b, 0)$, and $D \equiv (a, -b, 0)$. Here a and b denote yaw plane and vertical offsets for satellite-tether attachment points.

The pendulumlike auxiliary mass m, being much smaller than the satellite mass M, is treated as a particle. Transverse vibrations of thin tethers, made of a light but rigid material like Kevlar and assumed to have negligible mass, are ignored. Similarly, for the variable vector length $\boldsymbol{L}$ joining the auxiliary mass to satellite mass center S, two successive rotations, β about the x_0 axis referred to as

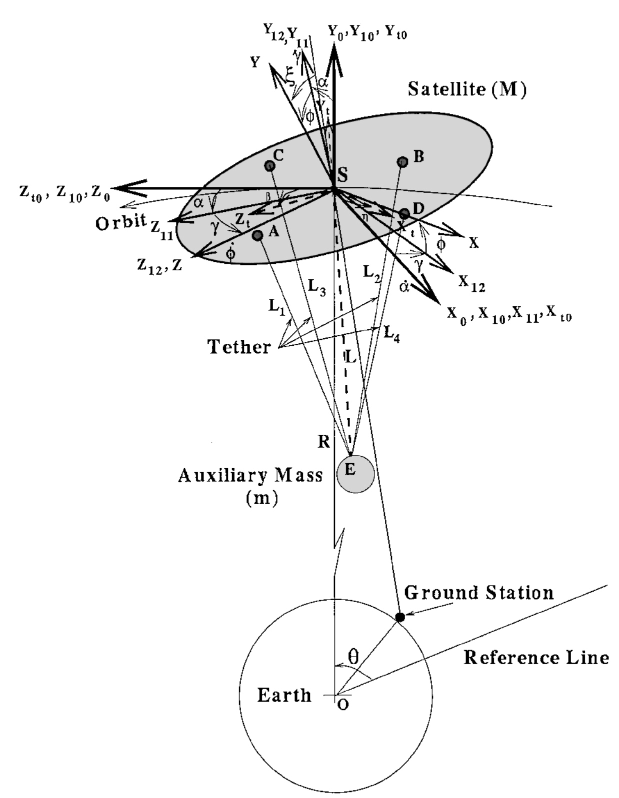

Fig. 1 Geometry of motion of TSS in inclined, 24-h circular orbits relative to an equatorial ground station.

Received 16 January 1998; revision received 2 October 1999; accepted for publication 14 October 1999.

*Professor, Department of Aerospace Engineering. Associate Fellow AIAA.

†Research Scholar; currently Science and Technology Agency Fellow, Flight Division, National Aerospace Laboratory, 6-13-1 Osawa Mitaka-shi, Tokyo 181, Japan.

the in-plane mass swing or pitch angle and η representing its out-of-plane swing or roll angle, lead to the associated tether coordinate frame $S - x_t y_t z_t$ with its y_t axis aligned along the $\boldsymbol{L}$ itself.

The governing Lagrangian equations of motion obtained after carrying out considerable algebraic manipulation and nondimensionalization may be written as[7]

$$\begin{aligned}
&\left\{\left[1 + \sin^2\phi(K_4 - 1)\right]\cos^2\gamma + K_5\sin^2\gamma\right\}\alpha'' + K_5\phi''\sin\gamma \\
&\quad - \tfrac{1}{2}(K_4 - 1)\sin 2\phi\,\gamma''\cos\gamma + (1 + \alpha')\left\{(K_4 - 1)\phi'\right. \\
&\quad \times \sin 2\phi\cos^2\gamma - \left.\left[1 + (K_4 - 1)\sin^2\phi - K_5\right]\sin 2\gamma\,\gamma'\right\} \\
&\quad + \gamma'[(1 - K_4)\phi'\cos 2\phi\cos\gamma - (1 - K_4)\gamma'\sin\phi\cos\phi\sin\gamma \\
&\quad + K_5\phi'\cos\gamma] - \tfrac{3}{2}\left[(K_4 + K_5 - 1)(\cos\alpha\sin\phi\right. \\
&\quad + \sin\alpha\sin\gamma\cos\phi)(-\sin\alpha\sin\phi + \cos\alpha\cos\phi\sin\gamma) \\
&\quad + (1 + K_4 - K_5)\sin\alpha\cos\alpha\cos^2\gamma - (1 - K_4 + K_5) \\
&\quad \times(\cos\alpha\cos\phi - \sin\alpha\sin\gamma\sin\phi)(\sin\alpha\cos\phi \\
&\quad + \left.\cos\alpha\sin\gamma\sin\phi)\right] - \sum_{j=1}^{4}\lambda_j\frac{\partial f_j}{\partial\alpha} = 0
\end{aligned} \tag{1}$$

$$\begin{aligned}
&[(1 - K_4)\sin\phi\cos\phi\cos\gamma]\alpha'' + \left[1 + (K_4 - 1)\cos^2\phi\right]\gamma'' \\
&\quad + \tfrac{1}{2}(1 + \alpha')(1 - K_4)(2\phi'\cos 2\phi\cos\gamma - \gamma'\sin 2\phi\sin\gamma) \\
&\quad + (1 - K_4)\gamma'\phi'\sin 2\phi + (1 + \alpha')[(1 + \alpha')\cos\phi\cos\gamma \\
&\quad + \gamma'\sin\phi]\cos\phi\sin\gamma + K_4[(1 + \alpha')\sin\phi\cos\gamma - \gamma'\cos\phi] \\
&\quad \times(1 + \alpha')\sin\phi\sin\gamma - K_5(1 + \alpha')[(1 + \alpha')\sin\gamma + \phi']\cos\gamma \\
&\quad + \tfrac{3}{2}\left[-(K_4 + K_5 - 1)(\cos\alpha\sin\phi + \sin\alpha\sin\gamma\cos\phi)\sin\alpha\right. \\
&\quad \times\cos\gamma\cos\phi + (1 + K_4 - K_5)\sin^2\alpha\sin\gamma\cos\gamma + (1 - K_4 \\
&\quad + \left.K_5)(\cos\alpha\cos\phi - \sin\alpha\sin\gamma\sin\phi)\sin\alpha\cos\gamma\sin\phi\right] \\
&\quad - \sum_{j=1}^{4}\lambda_j\frac{\partial f_j}{\partial\gamma} = 0
\end{aligned} \tag{2}$$

$$\begin{aligned}
&K_5\alpha''\sin\gamma + K_5(1 + \alpha')\gamma'\cos\gamma + K_5\phi'' + [(1 + \alpha')\sin\phi\cos\gamma \\
&\quad - \gamma'\cos\phi][(1 + \alpha')\cos\phi\cos\gamma + \gamma'\sin\phi] \\
&\quad - K_4[(1 + \alpha')\sin\phi\cos\gamma - \gamma'\cos\phi][(1 + \alpha')\cos\phi\cos\gamma \\
&\quad + \gamma'\sin\phi] - \tfrac{3}{2}[(K_4 + K_5 - 1)(\cos\alpha\sin\phi \\
&\quad + \sin\alpha\sin\gamma\cos\phi)(\cos\alpha\cos\phi - \sin\alpha\sin\gamma\sin\phi) \\
&\quad - (1 - K_4 + K_5)(\cos\alpha\cos\phi - \sin\alpha\sin\gamma\sin\phi) \\
&\quad \times(\cos\alpha\sin\phi + \sin\alpha\sin\gamma\cos\phi)] - \sum_{j=1}^{4}\lambda_j\frac{\partial f_j}{\partial\phi} = 0
\end{aligned} \tag{3}$$

$$\begin{aligned}
&\beta'' + 2(1 + \beta')\left(\frac{l'}{l} - \eta'\tan\eta\right) + 1.5\sin 2\beta \\
&\quad - \frac{1}{(l\cos\eta)^2}\sum_{j=1}^{4}\lambda_j\frac{\partial f_j}{\partial\beta} = 0
\end{aligned} \tag{4}$$

$$\begin{aligned}
&\eta'' + 2\eta'\frac{l'}{l} + 0.5[(1 + \beta')^2 + 3\cos^2\beta]\sin 2\eta \\
&\quad - \frac{1}{l^2}\sum_{j=1}^{4}\lambda_j\frac{\partial f_j}{\partial\eta} = 0
\end{aligned} \tag{5}$$

$$\begin{aligned}
&l'' - l[\eta'^2 + (1 + \beta')^2\cos^2\eta] + (1 - 3\cos^2\beta\cos^2\eta)l \\
&\quad - \sum_{j=1}^{4}\lambda_j\frac{\partial f_j}{\partial l} = 0
\end{aligned} \tag{6}$$

$$\lambda_j = C\epsilon_j U(\epsilon_j), \qquad j = 1, 4 \tag{7}$$

subject to the following constraints:

$$\begin{aligned}
f_j &= l_j - \left(\hat{a}^2 + \hat{b}^2 + l^2 - 2l\{\hat{a}_j[\cos\phi\cos\gamma\sin\eta\right. \\
&\quad - \sin\phi\cos\eta\cos(\alpha - \beta) - \cos\phi\sin\gamma\cos\eta\sin(\alpha - \beta)] \\
&\quad + \hat{b}[\sin\phi\cos\gamma\sin\eta + \cos\phi\cos\eta\cos(\alpha - \beta) \\
&\quad - \sin\phi\sin\gamma\sin(\alpha - \beta)] - \hat{c}_j[\sin\gamma\sin\eta \\
&\quad + \left.\cos\gamma\cos\eta\sin(\alpha - \beta)]\}\right)^{\frac{1}{2}} = 0, \qquad j = 1, \ldots, 4
\end{aligned} \tag{8}$$

Synthesis of Open-Loop Tether Length Control Laws

Here an attempt is made to compensate for the effect of longitudinal as well as lateral satellite drifts with respect to an equatorial ground station by ensuring line-of-sight-pointing stability for drifting satellites in nonequatorial, 24-h circular orbits through suitably controlled tether length variations. A simple geometric analysis is first carried out to obtain the effective satellite angular misalignment ξ with respect to the line of sight in terms of pitch, roll, and system parameters[11]:

$$\begin{aligned}
\xi = \cos^{-1}&\left\{[R_n\cos\alpha\cos\phi - \cos\phi\cos\theta\cos(\theta + \alpha)\right. \\
&\quad - \cos\phi\cos i_b\sin\theta\sin(\theta + \alpha) - \sin\phi\sin i_b\sin\theta] \Big/ \\
&\quad \left.\left[R_n^2 + 1 - 2R_n\left(\cos^2\theta + \sin^2\theta\cos i_b\right)\right]^{\frac{1}{2}}\right\}
\end{aligned} \tag{9}$$

where $R_n = R/R_{ea}$, R = orbital radius, and R_{ea} = Earth radius. Next we show that for achieving $\xi = 0$ the desired satellite pitch and roll variations are given by

$$\alpha = \tan^{-1}\left\{\frac{(1 - \cos i_b)\sin\theta\cos\theta}{\left[R_n - 1 + (1 - \cos i_b)\sin^2\theta\right]}\right\} \tag{10}$$

$$\phi = \sin^{-1}\left\{-\sin i_b\sin\theta\left[R_n^2 + 1 - 2R_n\left(\cos^2\theta + \sin^2\theta\cos i_b\right)\right]^{-\frac{1}{2}}\right\} \tag{11}$$

For the satellites positioned in an arbitrary equilibrium configuration, a substitution of the steady-state constant values for the variables $\alpha, \phi, \gamma, \beta, \eta, l$ and zero values for their derivatives into Eqs. (1–7) and considerable simplifying approximations and algebraic manipulations leads to the following relations:

$$\begin{aligned}
\beta &= \tfrac{1}{2}\sin^{-1}\left[(K_4 - K_5)\sin 2\alpha/l^2\right] \\
\eta &= \tfrac{1}{2}\sin^{-1}\left[(K_4 - 1)\sin 2\phi/l^2\right]
\end{aligned} \tag{12}$$

Strictly speaking, these relations apply to the fixed satellite equilibrium configuration. However, in view of rather slow rates of pitch and roll variations desired for the proposed satellite line-of-sight pointing stability, it may be justified to use these relations to at least first order of accuracy. On substitution of these expressions for α, ϕ, β, and η into Eqs. (8), we can show that the desired equilibrium satellite orientation can be achieved provided the tether lengths are regulated according to the following control laws:

$$\begin{aligned}
l_{j0} &= l_{t0} + (-1)^j\hat{a}\left[1 - (K_4 - K_5)/l_{t0}^2\right] \\
&\quad \times\tan^{-1}\left[\sin^2(i_b/2)\sin 2\theta/(R_n - 1)\right], \qquad j = 1, 2 \\
l_{j0} &= l_{t0} + (-1)^j\hat{a}\left[1 - (K_4 - 1)/l_{t0}^2\right] \\
&\quad \times\sin^{-1}[\sin i_b\sin\theta/(R_n - 1)], \qquad j = 3, 4
\end{aligned} \tag{13}$$

Table 1 Typical minimum tether length requirements for various satellite systems ($C = 10^7, \hat{a} = 0.1, \hat{b} = 0.2$)

System data	Small satellites	Medium satellites	Large satellites
(Satellite-auxiliary mass), kg	(500–25)	(1000–50)	(10^5–800)
(I_x–I_y–I_z), kg-m^2	(100–150–75)	(500–1000–500)	(10^7–10^7–8×10^6)
L_{ref}, m	4.5	4.5	115
$(L_{t0})_{\min}$, m			
$i_b = 5$ deg	9	9	230
$i_b = 20$ deg	14	14	345
$i_b = 45$ deg	17	17	460

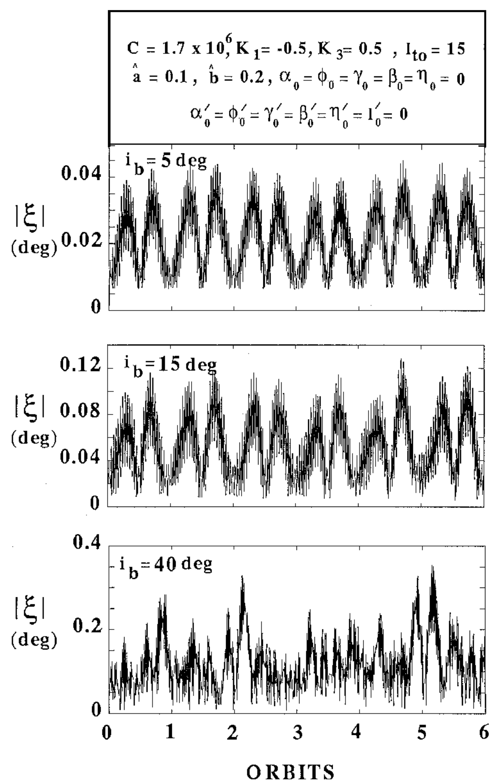

Fig. 2 Typical response plots showing maximum relative satellite attitude misalignments as affected by inclination i_b.

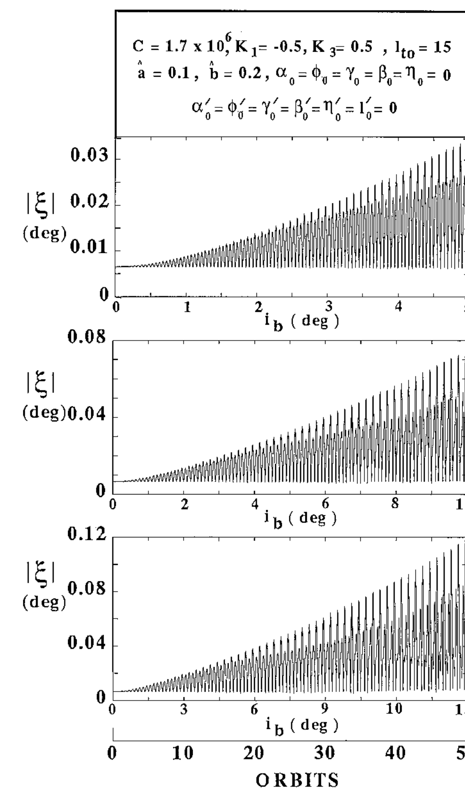

Fig. 3 Typical satellite response demonstrating the effectiveness of the controller for uniformly growing i_b.

Results and Discussion

With a view to assess the effectiveness of the proposed attitude control strategy, the detailed system attitude misalignment ξ response is numerically simulated using the exact Eqs. (1–8). The attitude response results presented here correspond to tether length variations in accordance with the open-loop control policy as given by Eqs. (13).

Figure 2 shows the line-of-sight misalignment errors ξ for orbital inclinations of 5, 15, and 40 deg. The resulting attitude misalignment errors are found to have rather low amplitudes of oscillations, which, in general, increase with inclination. The overall trends remain virtually unchanged regardless of the satellite mass distribution. Simulation of system attitude response for varying tether offsets in their feasible range showed that, in general, an increase in the value of offset $\hat{a}$ leads to improvement in satellite attitude behavior. In contrast, lower $\hat{b}$ values resulted in greater precision in ξ response.

An important adverse effect of environmental perturbations on the geosynchronous satellites is one of secular drift in their orbital inclination, which increases almost uniformly with time. Figure 3 presents the effect of rate of change of inclination for the drifting satellites on ξ response. As expected, the satellite misalignment continually grows with increasing inclination. The larger the drift rate of orbital inclination is, the larger the corresponding maximum satellite attitude misalignments would be. Even for the large changes in inclination of, e.g., 15 deg in 50 orbits at unrealistically high rates assumed, the maximum misalignments remain well within a small fraction of a degree.

The prior knowledge of minimum tether length requirement for the proposed control strategy is of considerable importance. This information, based on extensive numerical simulations over a range of tether lengths for some typical situations, is presented in tabular form (Table 1). The table covers practically all types of tethered satellite-auxiliary mass configurations.

Conclusion

In general, tether lengths needed to increase with an increase in the size of the satellite as well as a decrease in the auxiliary mass attached. The tether lengths on the order of a few meters may suffice to provide the desired attitude compensation to ensure the satellite line-of-sight-pointing for even relatively large north-south satellite drifts. The proposed variable attitude control approach may also be useful as an alternative to the conventional and perhaps more expensive station-keeping maneuvers required for geostationary satellites in contingencies and/or during last leg of the satellite missions with onboard fuel nearing depletion. The nearly passive nature of the proposed mechanism using short tethers along with small auxiliary mass needed makes the concept particularly attractive for future space missions.

References

[1] Kumar, K., Khosla, A., and Chaudhary, K., "Tether as Satellite Attitude Stabilizer in Elliptic Orbits: A Novel Concept," *Proceedings of AAA/AIAA Astrodynamics Conference*, 1993, pp. 859–875.

[2] Kumar, K., "Satellite Attitude Stabilization Through Tether," *Acta Astronautica*, Vol. 35, No. 6, 1995, pp. 385–390.

[3]Kumar, K., and Kumar, K. D., "Open-Loop Satellite Librational Control in Elliptic Orbits Through Tether," *Acta Astronautica*, Vol. 41, No. 1, 1997, pp. 15–21.

[4]Kumar, K., and Kumar, K. D., "Satellite Attitude Maneuver Through Tether: A Novel Concept," *Acta Astronautica*, Vol. 40, No. 2–8, 1997, pp. 216–224.

[5]Kumar, K., and Kumar, K. D., "Auto-Attitude-Stabilization of a Twin Satellite System Through Very Short Tethers," *Journal of Spacecraft and Rockets*, Vol. 35, No. 2, 1998, pp. 199–204.

[6]Kumar, K., and Kumar, K. D., "Passive Three-Axis Satellite Pointing Stability Through Tether," International Astronautical Federation, Paper IAF-97-A.3.02, Oct. 1997.

[7]Kumar, K., and Kumar, K. D., "Satellite Pitch and Roll Attitude Maneuvers Through Very Short Tethers," *Acta Astronautica*, Vol. 44, No. 5, 1999, pp. 257–265.

[8]Lavean, G. E., and Martin, E. J., "Communications Satellites," *Astronautics and Aeronautics*, Vol. 12, No. 1, 1974, pp. 54–61.

[9]Kumar, K., "Some Aspects Related to the Satellite Applications in Non-Stationary 24-Hour Orbits," *Acta Astronautica*, Vol. 9, No. 1, 1982, pp. 147–154.

[10]Akin, D. L., "Some Applications of Non-Stationary Geosynchronous Orbits," AIAA Paper 78-1407, Aug. 1978.

[11]Kumar, K., "A Solar Attitude Controller for Extending Operational Life-Span of Communication Satellites," *Acta Astronautica*, Vol. 17, No. 1, 1988, pp. 61–67.

J. D. Gamble
Associate Editor

Computing Geodetic Coordinates in Space

Yves Nievergelt*
Eastern Washington University, Cheney, Washington 99004-2431
and
Stephen P. Keeler†
The Boeing Company, Seattle, Washington 98124-2207

Nomenclature

a	= equatorial radius of the planet, m
b	= polar radius of the planet, m
$\mathcal{C}$	= section of the planet's surface by a plane containing the polar axis and $\boldsymbol{X}$
$\boldsymbol{C}(\alpha)$	= point on $\mathcal{C}$ with geodetic latitude α
e	= eccentricity of the planet, $e = \sqrt{(1-\sigma^2)}$ (dimensionless)
$H(\alpha)$	= distance from $\boldsymbol{X}$ to $\boldsymbol{C}(\alpha)$, m
h	= geodetic altitude of $\boldsymbol{X}$, m
$\boldsymbol{N}$	= outward unit normal vector at $\boldsymbol{P}$
$\boldsymbol{O}$	= center of the oblate spheroidal planet
$\boldsymbol{P}$	= intersection of the planet's surface and the line through $\boldsymbol{O}$ and $\boldsymbol{X}$
$\boldsymbol{Q}$	= intersection of the planet's equator and the line through $\boldsymbol{P}$ and $\boldsymbol{X}$
$\boldsymbol{X}$	= point in space whose geodetic coordinates are to be computed
(x, y, z)	= Cartesian (geocentric) coordinates of $\boldsymbol{X}$, m
$\beta_e(\alpha)$	= auxiliary function, $\sqrt{\{1-e^2[\sin(\alpha)]^2\}}$ (dimensionless)
$\theta(\alpha)$	= angle between $\boldsymbol{C}'(\alpha)$ and $\boldsymbol{C}(\alpha) - \boldsymbol{X}$, deg
κ	= contraction constant (dimensionless)
λ	= geodetic latitude of $\boldsymbol{X}$, deg
μ	= geocentric latitude of $\boldsymbol{X}$, that is, polar angle of the Cartesian point (ρ, z), deg
ρ	= polar radius of the Cartesian point (x, y), $\sqrt{(x^2+y^2)}$, m
σ	= ratio of the polar and equatorial radii, $\sigma = b/a$ (dimensionless)
ϕ	= geodetic latitude of $\boldsymbol{P}$, deg
φ	= longitude of $\boldsymbol{X}$, that is, polar angle of the Cartesian point (x, y), deg

Subscripts

d	= negative altitudes (deep), $h < 0$
h	= high altitudes (high), $a\sigma^2/\beta_e(\lambda) < h$
ℓ	= low altitudes (low), $0 \leq h \leq a\sigma^2/\beta_e(\lambda)$
$0, 1, n, n+1$	= number of iterations

Received 4 March 1999; revision received 10 September 1999; accepted for publication 9 November 1999.

*Professor, Department of Mathematics, MS-32.

†Manager, Geometry and Optimization Group, P.O. Box 3707, Mail Stop 7L-21.

Introduction

THIS Note presents a provably accurate algorithm to compute the geodetic latitude and geodetic altitude of a point in space relative to an oblate spheroid (a planet), given the geocentric position of the point relative to the spheroid. This computation is often necessary for navigation and tracking of aircraft, space vehicles, or other objects. The measurements yield the geocentric Cartesian coordinates (x, y, z) of the target $\boldsymbol{X}$:

$$\boldsymbol{X} = \begin{pmatrix} \rho \\ z \end{pmatrix} = \begin{Bmatrix} [a/\beta_e(\lambda) + h]\cos(\lambda) \\ [a\sigma^2/\beta_e(\lambda) + h]\sin(\lambda) \end{Bmatrix} \tag{1}$$

Equation (1) relates the cylindrical coordinates (ρ, z) to the geodetic coordinates (λ, h) (Ref. 1) (Fig. 1). The problem consists of computing the target's geodetic altitute h and geodetic latitude λ given x, y, z. This problem can be solved in closed form (contrary to Deprit and Deprit-Bartholome[2]) because it reduces to solving a quartic equation. However, a closed-form algebraic solution of the quartic equation is impractical for numerical computations for three reasons. First, it requires the computation of a complex cube root, which itself involves a numerical approximation. Second, algebraic solutions contain subtractions that can result in catastrophic cancellations of significant digits. Finally, because of the complexity of the algebraic solutions, no practical upper bounds on the effects of rounding errors, overflow, and underflow appear to exist. The literature contains various numerical approximations for the geodetic coordinates,[3] but apparently does not provide bounds on the errors in the presence of floating-point arithmetic or other perturbations, nor bounds on the number of iterations necessary to achieve a specified accuracy. In one instance, an algorithm[4] published in this journal attempts a division by zero above the poles and near the poles calls for divisions by small numbers that would amplify previous rounding or measurement errors.

In contrast, the algorithm presented here begins with a geocentric approximation and refines it through one iteration of a contracting map. The method is accurate to two-millionths of a degree for

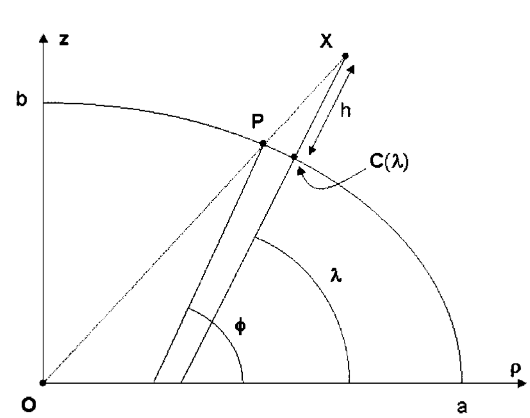

Fig. 1 Problem: given ρ and z for X, compute h and λ.